ANNALES
UNIVERSITATIS MARIAE CURIE - SKLODOWSKA
LUBLIN — POLONIA
VOL. XLIII/XLIV, 6 SECTIO AAA 1988/1989

Friedrich-Schiller-Universität Jena

K. GÄRTNER, W. WESCH, G. GÖTZ

Investigation of the Temperature Dependence of Axial Dechanneling by Point Defects

Calculations of the depth dependence of the Rutherford backscattering minimum yield were performed for crystals with non-correlated displaced lattice atoms (point defects). The main result is that the slope of the temperature dependence changes considerably for different displacement distances r_a. In order to explain this effect the contributions of the different dechanneling processes to the minimum yield are discussed in detail. It is shown that the combined action of these processes is quite different for different values of r_a which is responsible for the strong influence of the value of r_a on the temperature dependence of the minimum yield. This effect can be used for the analysis of point defects with preferred positions in the lattice cell. For example defects in N implanted GaAs are analysed.

1. Introduction

For about 20 years channeling has been used for defect studies in crystals [1-9]. The relative Rutherford backscattering yield for ions incident parallel to a crystal axis (RBS minimum yield χ_{min}) is increased if the crystal contains defects (displaced lattice atoms). The enhancement of the minimum yield is caused by direct backscattering and dechanneling of the ions due to the interaction with the displaced lattice atoms. The dechanneling mechanisms are different for different kinds of defects which are characterized by different correlations between the displacements of the lattice atoms. This paper deals with uncorrelated displaced lattice atoms (point defects, small defect clusters). With respect to dechanneling point defects (and small clusters) are characterized by the relative number n_{pd} of lattice atoms which are displaced from their lattice sites and by their displacement distance r_a perpendicular to the channeling direction (assumption of cylindrical symmetry is mostly justified). Only in the case where r_a can be assumed to be randomly distributed within the area belonging to one atomic string (heavily damaged crystals) the defect density $n_{pd}(z)$ can be calculated directly from the minimum yield $\chi_{min}(z)$ measured as a function of the depth z [1,2,3,7]. Otherwise, additional information is necessary for the determination of both the defect density $n_{pd}(z)$ and the distribution of the displacement distances r_a. Diffusion model calculations of Matsunami et al. [10,11] proved the temperature and energy dependence of dechanneling to depend on the value of r_a. This offered the possibility of a quantitative defect analysis by performing RBS measurements at different temperatures and different energies. More detailed investigations using a discontinuous model [7] showed that only the temperature dependence of dechanneling provides a useful information about the distribution of r_a. Therefore, the temperature dependence of axial dechanneling in crystals with non-correlated displaced lattice atoms is of special interest in this paper. The investigations are performed assuming all displaced lattice atoms to have the same value of the displacement distance r_a (r_a δ-distributed). This corresponds to point defects with prefer-

red positions in the lattice cell which appear mainly in weakly damaged crystals. The results are discussed and applied to the analysis of defects in Si and GaAs.

2. Dechanneling model

The model used is described in ref.[7] and in the following it is referred to as the discontinuous model. It is based on the general description of dechanneling given by Lindhard [12]. Instead of a continuous distribution $g(E_\perp, z)$ of the transverse energy $E_\perp$ of the ions at depth z the relative number $g_i(z)$ of ions with transverse energy between $E_{\perp i-1}$ and $E_{\perp i}$ ($E_{\perp i} = E_{\perp c}\, i/(i_{max}-i)$, $i=1,\ldots i_{max}$, see ref.[7]) is the physical quantity of interest. It is determined by a system of differential equations (master equation)

$$\frac{dg_i(z)}{dz} = \sum_j Q_{ij} g_j(z), \tag{1}$$

where the dechanneling matrix Q_{ij} is given by the probability per depth P_{ij} for the transition of an ion from group j to group i

$$Q_{ij} = P_{ij} - \delta_{ij} \sum_k P_{kj}. \tag{2}$$

The Rutherford backscattering minimum yield χ_{min} is obtained by

$$\chi_{min}(z) = \sum_i \pi_i g_i(z), \tag{3}$$

where π_i is the relative probability for hitting a regular lattice atom or a displaced atom [7]. The dechanneling matrix is the sum of all contributions from statistically independent processes (electronic scattering, nuclear scattering, scattering on point defects)

$$Q_{ij} = Q_{ij}^{(e)} + [1-n_{pd}(z)]Q_{ij}^{(n)} + n_{pd}(z)Q_{ij}^{(pd)}(r_a) \tag{4}$$

The calculation of $Q_{ij}^{(e)}$, $Q_{ij}^{(n)}$ and $Q_{ij}^{(pd)}(r_a)$ is described in ref.[7]. Note that the dechanneling matrix contribution of the point defects depends on the displacement distan-

ce r_a.

3. Temperature dependence of dechanneling

The temperature dependence of dechanneling is quite different for different values of r_a. This is demonstrated in fig.1a for the example of 1 MeV H^+ channeling in <111>Si with 10% of

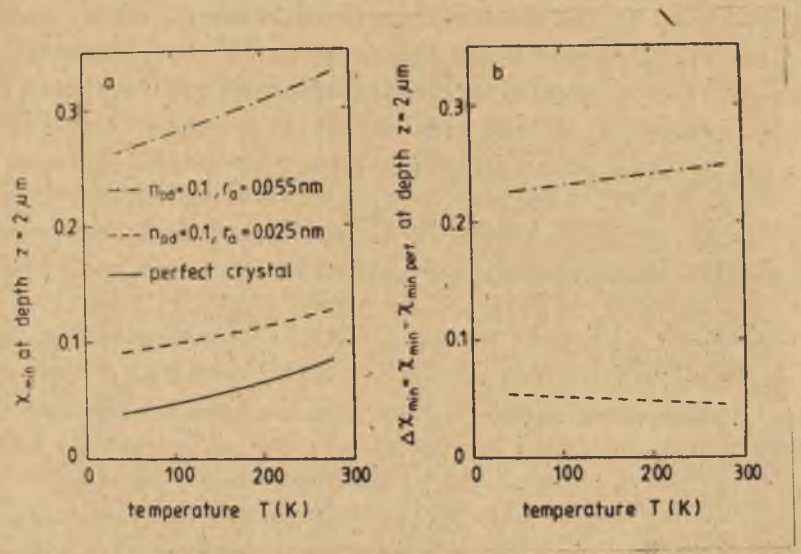

Fig.1. Temperature dependence of χ_{min} (fig.1a) and $\Delta\chi_{min}$ (fig.1b) at depth z = 2 µm for 1 MeV H^+ incident on perfect <111> Si and <111> Si with different point defects.

the lattice atoms being displaced by r_a = 0.025 nm and r_a = 0.055 nm, respectively. Of course, in all cases the minimum yield χ_{min} increases with respect to the minimum yield for the perfect crystal (n_{pd} = 0). However, the temperature dependence of χ_{min} is weaker or stronger than that of the perfect crystal for r_a = 0.025 nm or r_a = 0.055 nm, respectively. This can be seen more pronounced in fig.1b which shows the difference of the minimum yields $\Delta\chi_{min} = \chi_{min} - \chi_{min,perf}$. The slope of $\Delta\chi_{min}$ depends considerably on the value of r_a, and it changes even its sign. An explanation of this effect is given in the following.

The dechanneling contributions due to the scattering of the ions at the electrons (e), at the thermally vibrating lattice atoms (nuclear scattering, (n)), and at the displaced lattice atoms (point defects, (d)) are demonstrated in fig.2.

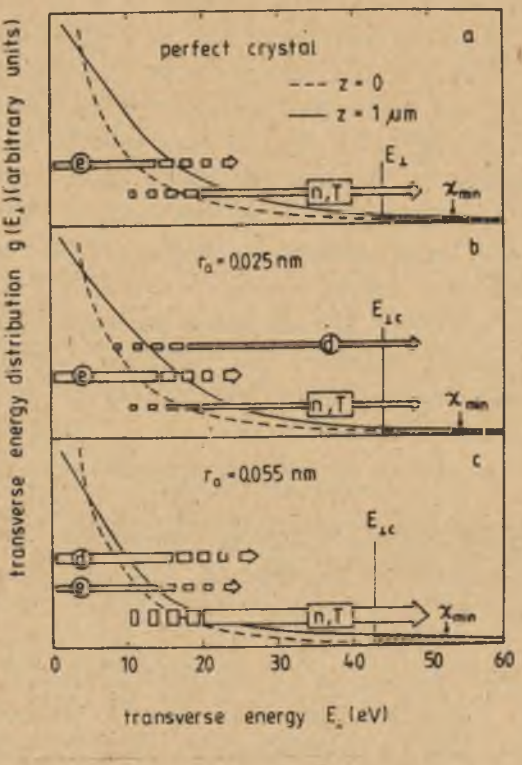

Fig.2. Transverse energy distributions at depth z = 0 and z = 1/um for 1 MeV H^+ incident on perfect <111> Si (fig.2a) and on <111> Si with 10% lattice atoms being displaced by r_a = 0.025 nm (fig.2b) and by r_a = 0.055 nm (fig.2c). The temperature is 160K in all cases. For the demonstration of the different dechanneling processes by the arrows see the text.

In the transverse energy concept dechanneling means the change of $E_\perp$ by the processes mentioned above. For a qualitative discussion the minimum yield can be estimated by

$$\chi_{min}(z) \approx \int_{E_{\perp c}}^{\infty} dE_\perp g(E_\perp, z), \qquad (5)$$

where $E_{\perp c} = \frac{1}{2} E \psi_1^2$ is the critical transverse energy (ψ_1 is the critical angle introduced by Lindhard).

The initial transverse energy distribution (z = 0) is heavily peaked at small transverse energies. Due to dechanneling the transverse energy distribution changes with increasing depth. However, small $E_\perp$ are still dominating. The situation for z = 1/um is shown in fig.2. It can be seen that in all three cases the enhancement of the minimum yield with increasing depth is caused by the reduction of the peak of $g(E_\perp)$ at small $E_\perp$. Therefore, with respect to dechanneling the main effect is the transverse energy transition from $E_\perp << E_{\perp c}$ to $E_\perp > E_{\perp c}$. This is provided by the three processes (e), (n), and (d) mentioned above. However, the relative contributions of these processes are different for different transverse energy regions and for different values of r_a. This is demonstrated in fig.2 by arrows of different positions, lengths, and thicknesses.

(i) Perfect crystal: For small $E_\perp$ the transverse energy is changed mainly by electronic scattering. The contribution of nuclear scattering is less by about two orders of magnitude (ions with small E do not reach the thermally vibrating lattice atoms). The changes of $E_\perp$ due to electronic scattering are small. Therefore, the electronic processes are effectiv only in a small $E_\perp$ region up to medium transverse energies (see arrow (e) in fig.2a). With increasing $E_\perp$ the nuclear processes dominate more and more. Their effective $E_\perp$ region (arrow (n,T) in fig.2a) increases to lower $E_\perp$ for increasing temperature. In summary, the enhancement of the minimum yield χ_{min} is the result of the combined action of the electronic and nuclear scattering processes. The temperature dependence of χ_{min} is introduced by the nuclear processes.

(ii) Crystal with slightly displaced lattice atoms (e.g. r_a = C.025 nm): In comparison with the perfect crystal (i) there are additional scattering processes at the displaced lattice atoms. For small displacement distances ($r_a \gtrsim$ thermal vibration amplitude) the effective $E_\perp$ region for ion scattering at the displaced lattice atoms is similar to that for

nuclear scattering. With increasing r_a this region extends to lower $E_\perp$ (arrow (d) in fig.2b). The influence of the additional thermal vibration of the displaced lattice atoms on the dechanneling was shown to be negligible for $r_a = 0.025$ nm. Therefore, the scattering at these defects is approximately independent of the temperature. For small $E_\perp$ the transverse energy is changed only by electronic processes as in the case of the perfect crystal. The further enhancement of the transverse energy up to $E_\perp > E_{\perp c}$ is provided by the nuclear scattering (n) and by the scattering at the defects (d). As it is expressed by the thicknesses of the arrows the resulting minimum yield in fig.2b is larger than that of the perfect crystal (fig.2a), but its contribution (n) from the scattering at the thermally vibrating lattice atoms is less than in the case of the perfect crystal. Therefore, the temperature dependence of χ_{min} for crystals with slightly displaced lattice atoms is weaker than that for the perfect crystal as shown in fig.1 (negative temperature dependence).

(iii) Crystals with heavily displaced lattice atoms (e.g. $r_a = 0.055$ nm): Defects with large displacement distances $r_a \approx 0.05 - 0.10$ nm interact preferentially with ions of small transverse energy. Therefore, their effective $E_\perp$ region is similar to that of electronic scattering (fig.2c). This causes much more ions with small $E_\perp$ to increase their transverse energy than in the case of the perfect crystal. The further enhancement of the transverse energy up to $E_\perp > E_{\perp c}$ is obtained only by nuclear processes. Because of the large transverse energy transfer for small $E_\perp$ the nuclear processes are much more effective than they are in the perfect crystal. Therefore, in this case χ_{min} is much larger and the temperature dependence of χ_{min} is stronger than for the perfect crystal according to the results depicted in fig.1.

4. Application to defect analysis

As shown in chapter 3 the temperature dependence of $\Delta\chi_{min} = \chi_{min} - \chi_{min,perf}$ is quite different for different values of r_a. Therefore, both $n_{pd}(z)$ and r_a can be determined from $\Delta\chi_{min}(z,T)$ measured for different temperatures. The

procedure is described in the following.

In the first step the difference of the minimum yields $\Delta\chi_{min}(z,T_f)$ is measured for a fixed temperature T_f. Assuming a set of different values of r_a the corresponding defect densities $n_{pd}(z)$ are calculated from $\Delta\chi_{min}(z,T_f)$. The result is a set of (r_a, $n_{pd}(z)$). In the second step $\Delta\chi_{min}(z,T)$ is calculated for different temperatures using the set of (r_a, $n_{pd}(z)$). The calculated temperature dependence of $\Delta\chi_{min}$ is quite different for different (r_a, $n_{pd}(z)$). The comparison with $\Delta\chi_{min}(z,T)$ measured for $T \neq T_f$ provides the correct r_a and $n_{pd}(z)$. In order to get sufficient accuracy measurements should be performed in a temperature interval of 100K at least.

In fig.3 and 4 this method is demonstrated for the example of He implanted silicon using T_f = 160K. The calculated temperature dependences of $\Delta\chi_{min}$ at depth z = 2/um for different

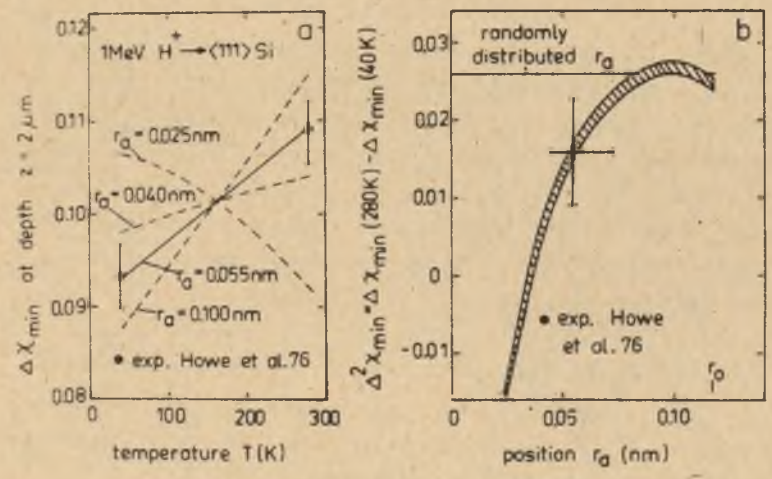

Fig.3. Temperature dependence of the calculated $\Delta\chi_{min}$ at depth z = 2/um for different values of r_a (fig.3a) and $\Delta^2\chi_{min}$ at depth z = 2/um as a function of r_a (fig.3b) for 1 MeV H^+ incident on He implanted <111> silicon. The calculated curve $\Delta^2\chi_{min}(r_a)$ contains the statistical error introduced by simulation. For the experimental data see fig.4.

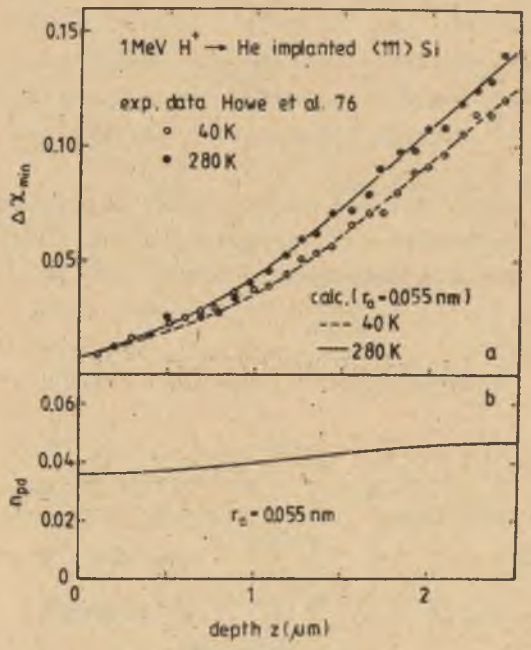

Fig.4. Depth dependence of the measured and calculated $\Delta\chi_{min}$ at temperatures of 40K and 280K for 1 MeV H^+ incident on <111> silicon implanted with 2 MeV He ions ($3.6*10^{16}$ cm^{-2}, 40K) and annealed at 290K for 10 min (fig.4a) and the depth dependence of the point defect density n_{pd} calculated for r_a = 0.055 nm (fig.4b).

values of r_a (and the corresponding $n_{pd}(z)$, not shown) are depicted in fig.3a. The comparison with the experimental data of Howe et al.[13] provides r_a = 0.55 nm. For the estimation of the error the second difference $\Delta^2\chi_{min} = \Delta\chi_{min}(2\,\mu m, 280K) - \Delta\chi_{min}(2\,\mu m, 40K)$ as a measure of the slope of the temperature dependence of $\Delta\chi_{min}$ is a more useful quantity (see fig.3b). It can be seen that $\Delta^2\chi_{min}$ depends heavily on r_a for $r_a \lesssim 0.07$ nm. For $r_a > 0.07$ nm $\Delta^2\chi_{min}$ changes weakly and is approximately equal to the value obtained for r_a randomly distributed within the area belonging to one atomic

string. Therefore, the method considered is very sensitive for point defects with small and medium displacement distances ($r_a \lesssim 0.07$ nm for <111>Si). Fig.4 shows the functions $n_{pd}(z)$, $\Delta\chi_{min}(z,40K)$, and $\Delta\chi_{min}(z,280K)$ calculated for $r_a = 0.055$ nm and the corresponding experimental data. The good agreement for the two temperatures is obtained only for this value of r_a.

As a second example point defects in <100>GaAs implanted with 280 keV N at room temperature are investigated for different nitrogen doses. The results obtained for $7*10^{13}cm^{-2}$ N implantation are depicted in fig.5a and 6 (T_f = 295K).

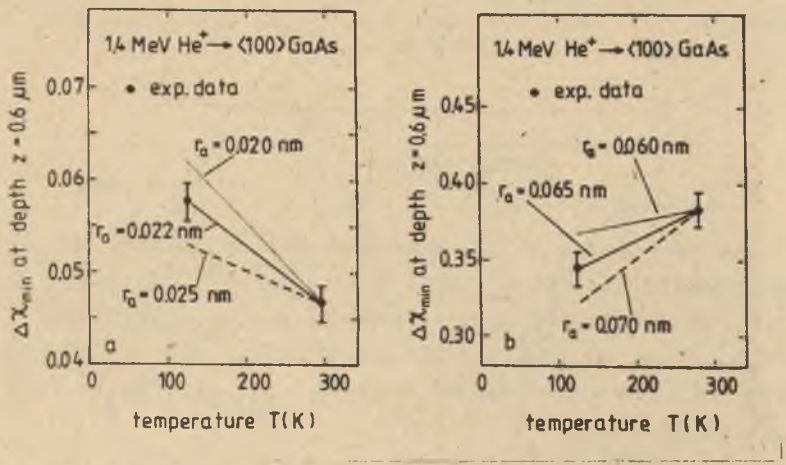

Fig.5. Temperature dependence of $\Delta\chi_{min}$ calculated for different values of r_a measured with 1.4 MeV He^+ incident on <100>GaAs implanted at room temperature with $7*10^{13}Ncm^{-2}$ (fig.5a) and with $10^{16}Ncm^{-2}$ (fig.5b).

They proof the existence of a negative temperature dependence of $\Delta\chi_{min}$. The comparison of the measured and calculated temperature dependence of $\Delta\chi_{min}$ provides $r_a = 0.022$ nm. The corresponding calculated $n_{pd}(z)$ and $\Delta\chi_{min}(z,T)$ are given in fig.6. For the higher dose of $10^{16}Ncm^{-2}$ the results (figs.5b

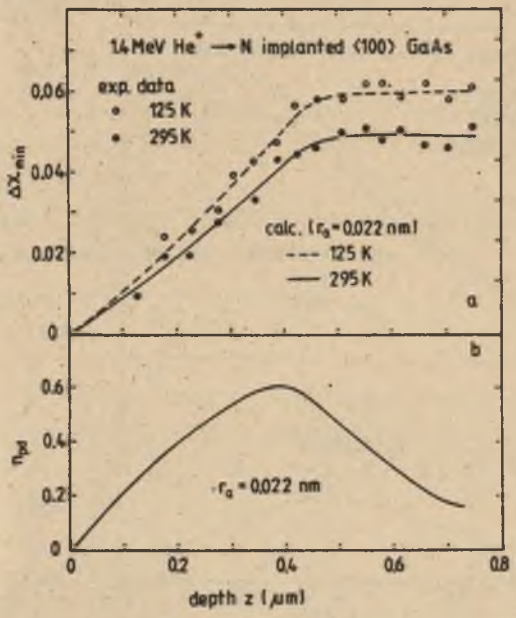

Fig.6. Depth dependence of the measured and calculated $\Delta\chi_{min}$ at temperatures of 125K and 295K for 1.4 MeV He^+ incident on <100>GaAs implanted at room temperature with $7*10^{13}Ncm^{-2}$ (fig.6a) and the depth dependence of n_{pd} calculated for r_a = 0.022 nm (fig.6b).

and 7, T_f = 295K) show a positive temperature dependence of $\Delta\chi_{min}$ providing r_a = 0.065 nm. The corresponding calculated $n_{pd}(z)$ and $\Delta\chi_{min}(z,T)$ are depicted in fig.7. These results indicate that the N implantations with different doses cause different point defect complexes which are characterized by different displacement distances r_a. Possible defect complexes are discussed in ref.[14].

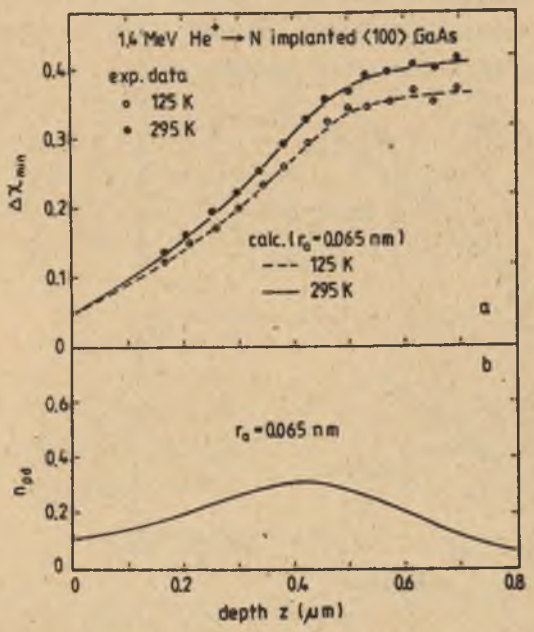

Fig.7. Depth dependence of the measured and calculated $\Delta\chi_{min}$ at temperatures of 125K and 295K for 1.4 MeV He^+ incident on <100>GaAs implanted at room temperature with 10^{16}Ncm^{-2} (fig.7a) and the depth dependence of n_{pd} calculated for r_a = 0.065 nm (fig.7b).

References

[1] Bógh E.: Can. J. Phys. 46 (1968) 653.
[2] Westmoreland J. E., Mayer J. W., Eisen F. H., Welch B.: Rad. Eff. 6 (1970) 161.
[3] Picraux S. T.: J. Appl. Phys. 44 (1973) 587.
[4] Appleton B. R.: Defects in semiconductors, Proc. Materials Research Society Annual Meeting, Boston 1980, (North-Holland, Amsterdam, 1981) p. 97.
[5] Chu W. K.: ibid., p. 117.
[6] Picraux S. T.: ibid., p. 135.
[7] Gärtner K., Hehl K., Schlotz-hauer G.: Nucl. Instr. and Meth. 216 (1983) 275, B4 (1984) 55 and B4 (1984) 63.
[8] Gärtner K., Hehl K.: Nucl. Instr. and Meth. B12(1985) 205.
[9] Gärtner K., Uguzzoni A.: Nucl. Instr. and Meth. B33 (1988) 607.
[10] Matsunami N., Gotoh T., Itoh N.: Rad. Eff. 33 (1977) 209.
[11] Matsunami N., Gotoh T., Itoh N.: Nucl. Instr. and Meth. 149 (1978) 430.
[12] Lindhard J., Dan K.: Vid. Selsk. Mat. Fys. Med. 34 (1965) no. 14.
[13] Howe I. M., Swanson M. I., Quenneville A. F.: Nucl. Instr. and Meth. 132 (1976) 241.
[14] Wesch W., Jordanov A., Gärtner K., Götz G.: Nucl. Instr. and Meth. B39 (1989) 445.